Original Paper

Brain, Behavior and Evolution

Brain Behav Evol
DOI: 10.1159/000438448

Received: March 12, 2015
Returned for revision: April 15, 2015
Accepted after second revision: July 7, 2015
Published online: September 9, 2015

Visual Capability of the Weakly Electric Fish *Apteronotus albifrons* as Revealed by a Modified Retinal Flat-Mount Method

Tomo Takiyama[a] Valdir Luna da Silva[a, b] Daniel Moura Silva[b]
Sawako Hamasaki[a] Masayuki Yoshida[a]

[a]Graduate School of Biosphere Science, Hiroshima University, Higashihiroshima, Japan; [b]Biologic Science Center, Pernambuco State Federal University (UFPE), Recife, Brazil

Key Words
Apteronotus albifrons · Electric fish · Retinal flat mount · Vision

Abstract
Apteronotus albifrons (Gymnotiformes, Apteronotidae) is well known to have a sophisticated active electrosense system and is commonly described as having poor vision or being almost blind. However, some studies on this species suggest that the visual system may have a role in sensing objects in the environment. In this study, we investigated the visual capabilities of *A. albifrons* by focusing on eye morphology and retinal ganglion cell distribution. The eyes were almost embedded below the body surface and pigmented dermal tissue covered the peripheral regions of the pupil, limiting the direction of incoming light. The lens was remarkably flattened compared to the almost spherical lenses of other teleosts. The layered structure of the retina was not well delineated and ganglion cells did not form a continuous sheet of cell bodies. A newly modified retinal flat-mount method was applied to reveal the ganglion cell distribution. This method involved postembedding removal of the pigment epithelium of the retina for easier visualization of ganglion cells in small and/or fragile retinal tissues. We found that ganglion cell densities were relatively high in the periphery and highest in the nasal and temporal retina, although specialization was not so high (approx. 3:1) with regard to the medionasal or mediotemporal axis. The estimated highest possible spatial resolving power was around 0.57 and 0.54 cycles/degree in the nasal and temporal retina, respectively, confirming the lower importance of the visual sense in this species. However, considering the hunting nature of *A. albifrons,* the relatively high acuity of the caudal visual field in combination with electrolocation may well be used to locate prey situated close to the side of the body.

Introduction

The Gymnotiform order of electric fishes is a diverse and important group in South and Central American water environments. Although electric fish species comprise only 3% of the fish biodiversity in tropical regions, some studies have suggested that they account for the majority (>80%) of the fish biomass in many aquatic environments in the Amazonia [Marrero and Taphorn, 1991; Cox-Fernandes, 1998]. There are at least 135 species and most of them belong to the Apteronotidae family [Albert, 2003; Albert and Crampton, 2005]. The diversity of species is reflected in the variety of ecological niches and behaviors.

0006–8977/15/0000–0000$39.50/0

E-Mail karger@karger.com
www.karger.com/bbe

Masayuki Yoshida
Graduate School of Biosphere Science
Hiroshima University
Kagamiyama 1-4-4, Higashihiroshima, Hiroshima 739-8528 (Japan)
E-Mail yosidam@hiroshima-u.ac.jp

Some species are aggressive predators, others are planktivores, and at least one species eats freshwater sponges [Albert, 2003].

Many apteronotid fishes inhabit the Amazon floodplain, while some are more specialized in occupying deeper portions of the river channel. They have small eyes and are commonly described as having poor vision or being almost blind [Albert, 2003]. Apteronotid fishes have been used as model animals to investigate active electrosense and electrocommunication, but almost no attention has been paid to their sense of vision. The black ghost *Apteronotus albifrons,* like many other electric fishes living in dark environments and/or having nocturnal lifestyles, has been suggested to rely predominantly on its active electrosense to sense its surroundings [Giassi et al., 2011; Lavoué et al., 2012], and it is expected to have poorly developed visual capabilities [Landsberger et al., 2008]. The eyes of *A. albifrons* are small and apparently less developed compared to those of other fish species for which vision is more important [Sas and Maler, 1986].

Nevertheless, a limited number of studies have shown that vision plays a role to some extent even in the presence of electroreception [Bastian, 1982; Sas and Maler, 1986]. Retinofugal projections in *A. albifrons* show a remarkable similarity to those in nonelectroreceptive teleosts [Sas and Maler, 1986], suggesting the relevance of vision in this species. In addition, it has been shown that information about electroreception and vision converges at the optic tectum in *A. albifrons* and that visual information can strongly affect electrosensory responses [Bastian, 1982]. It has been reported in the Gymnotiform *Sternopygus* (Sternopygidae) that object tracking is markedly impaired by restriction of visual as well as electrosensory information [Rose and Canfield, 1993].

To further understand the sensory ecology of Gymnotiform electric fishes, which have been mainly recognized as models for studying electroreception, it is important to closely investigate other sensory modalities including vision. In this study, we aimed to gain insight into the visual capabilities of *A. albifrons* by focusing on the anatomy of the eyes and the topographic arrangement of retinal neurons.

Topographic mapping of retinal ganglion cells is established as a powerful tool for evaluating the visual acuity of animals including fishes and for comparative studies of visual capabilities [Collin, 2008; Moore et al., 2012]. The shape and location of the retinal region where ganglion cells are present at a high density have been known to reflect the visual ecology of the animal and are called retinal specialization [Collin and Pettigrew, 1988; Browman et al., 1990; Collin, 2008; Moore et al., 2012]. The region where ganglion cells show a localized increase is called the area centralis [Hughes, 1977; Collin and Pettigrew, 1988; Collin and Partridge, 1996]. The image projected to this region is considered to be processed at a relatively higher spatial resolution. A horizontally extended high-ganglion-cell-density region forms a visual streak, which is typically developed in animals with a high demand for horizontal viewing of the plane area [Hughes, 1971, 1977; Collin and Pettigrew, 1988]. The retinal flat-mount, or whole-mount, technique has been commonly used to examine the morphology and distribution of retinal cells including ganglion cells and to assess various visual parameters [Ullmann et al., 2012]. Several methods of retinal flat-mount preparations to examine the topographic distribution of neuronal elements in retinae have been developed [for a review, see Collin, 2008; Ullmann et al., 2012]. Surgical removal [Graydon and Giorgi, 1984; Collin and Pettigrew, 1988; Mangrum et al., 2002; Ullmann et al., 2012; Muguruma et al., 2013] or chemical bleaching [Oliveira et al., 2006; Ullmann et al., 2012] of the pigment epithelium is usually required for observation with a conventional microscope using transmitted light [Ullmann et al., 2012].

However, it is technically difficult to apply these conventional methods to small [Ullmann et al., 2012] or less-developed eyes with fragile retinal tissues in some fish species, including *A. albifrons*. Examination of small eyes requires a time-consuming complex method involving reconstruction of the sectioned material to estimate the topographic arrangement of retinal cells [Ullmann et al., 2012]. This technical difficulty has limited comparative and ontogenetic studies of visual functions, especially in fishes with small eyes.

There are many small fishes and small-eyed fishes (e.g. electric fishes) adapted to various ecological niches. In addition, the morphology and function of the visual system are required to be tuned appropriately as the body size and lifestyle dramatically change during ontogeny in fishes [Shand et al., 2000]. Thus, comparative and ontogenetic studies of retinal morphologies in certain species can contribute to further understanding the adaptive mechanisms of vision.

Here we developed a novel simple method for flat-mount preparations suitable for examining retinal ganglion cell topography in small and/or fragile retinae. We used this technique together with conventional histological methods to examine the gross anatomy of eyes and the topographic arrangement of retinal ganglion cells in *A. albifrons* to reveal the visual capability of this species.

Materials and Methods

Animals

The 7 black ghost *A. albifrons* used in the experiment were obtained from a local supplier. One individual (total length 133.6 mm) was used for observation of the external morphology of the head and eye, 3 (total lengths 93.3, 96.6, and 106.6 mm) were used for retinal flat-mount preparation, and the other 3 (total lengths 92.7, 97.5, and 106.4 mm) were used for histological sectioning to examine eye morphology. The fishes were deeply anesthetized using an overdose of 2-phenoxyethanol, decapitated, and fixed in Davidson's fixative for 3 h or overnight at room temperature. The pilot experiment revealed that the shrinkage of the eye of *A. albifrons* during overnight fixation in Davidson's fixative was 7.52 ± 4.43% (mean ± SEM, n = 5 from 3 animals).

All animal experiments were conducted in accordance with the Guidelines for Animal Experimentation of Hiroshima University.

Retinal Flat Mount and Histological Sectioning of the Eye

Four retinae from 3 *A. albifrons* were used to make flat-mount preparations. A small radial incision was made in the ventral margin of the eye to keep track of the orientation of the tissue during the following procedure. The iris was cut away and the lens was removed. Then the eye cup was excised from the head and 5 peripheral radial cuts were made. The extrinsic ocular muscles and the sclera were removed. Then the retina with the choroid and the pigment epithelium still attached was flattened with its optic nerve layer uppermost on a piece of nylon mesh (opening 45 μm, thread diameter 40 μm; Tanaka Sanjiro, Fukuoka, Japan), which was laid on a stainless-steel plate (30 mm wide, 15 mm deep, and 1 mm thick). Another piece of nylon mesh and a stainless-steel plate were placed on the retina. The latter stainless-steel plate had a hole slightly larger than the retina so that the solutions could penetrate the tissue through the mesh. Care was taken to keep the tissue and the mesh wet with phosphate-buffered saline during the procedure. The stainless-steel plates were securely held to each other using a clip. Thus the retina was kept flattened between the mesh during the following staining and dehydration processes.

Each retina was then rinsed thoroughly with 0.1 M phosphate buffer and Nissl stained in a solution containing 0.5% cresyl violet and 0.2% acetic acid for 1–2 h with agitation at room temperature. The stained tissue was rinsed twice with distilled water and once with 70% ethanol, and then soaked in 100% ethanol for 10 min. The tissue was then rinsed with acetone and completely dehydrated with 2 changes of fresh acetone for 10–20 min each. After dehydration, the mesh and stainless-steel plates were removed in acetone and the acetone was substituted with epoxy resin (WN-08; Epoch, Osaka, Japan). The container with the retina and resin was enclosed in a deaeration tank and deaerated for 3–5 h to facilitate the substitution.

A piece of tracing paper (thickness 0.15 mm) with a hole in its center was put on a cover glass. The retina was placed in the paper hole on the cover glass with the pigment epithelium layer facing upwards, and a small amount of resin was poured onto the tissue. The cover glass was then sandwiched between a pair of silicone plates held together with a clip. After complete hardening of the resin, the silicone plates were carefully removed.

The cover glass onto which the resin-embedded preparation was attached was mounted in a petri dish using small pieces of adhesive tape and covered with water. Under a stereoscopic microscope equipped with transmission illumination from below, the pigment epithelium was scraped using a handheld router (No. 28600; Kiso Power Tool, Osaka, Japan) equipped with a fine bit (No. 26712; Kiso Power Tool). Nissl-stained neural elements in the retina area were used to identify the pigment epithelium layer for removal. In addition, the progress of the scraping could be checked at any stage under a conventional microscope by mounting the specimen onto a glass slide with water. The scraping procedure was continued until the inner nuclear layer was exposed. Although complete removal of the inner nuclear layer yielded better visualization of the ganglion cells, it was safer to leave at least the inner part of the inner nuclear layer to ensure that the whole ganglion cell layer was included in the preparation. The specimen was then dried and mounted onto a glass slide with the epoxy resin.

In the pilot experiment, to examine the validity of the new retinal flat-mount method, this method was applied to small eyes (diameter 0.82 mm) in a zebrafish juvenile (standard length 7.5 mm). We found that the quality of the flat-mount preparations was sufficient to measure ganglion cell densities at suitable locations over the retina and to build a retinal ganglion cell topographical map. We also confirmed that ganglion cell topographical maps in juvenile zebrafishes obtained from flat-mount preparations made using the present method were consistent with that reported in a previous work in which a conventional retinal flat-mount method was used [Mangrum et al., 2002].

Ganglion cells were counted to examine the pattern of distribution in more than 110 microregions over the retina, and the cell densities at these regions were calculated. Isodensity contour maps of the retinal ganglion cell distribution were made using statistical analysis software R (version 3.0.2; http://www.r-project.org).

To examine the anatomy of the eye and the layered structure of the retina, histological sections of the eye together with surrounding tissues were made from 3 individuals of *A. albifrons*. The fishes were deeply anesthetized, decapitated, and fixed in Davidson's fixative. The fixed head was washed in phosphate-buffered saline for 2 h and immersed in 0.2% toluidine blue in 0.1 M phosphate buffer for 2 days. The stained tissue was washed in deionized water, dehydrated, and embedded in the epoxy resin. Serial horizontal sections (3–5 μm) of the eye and surrounding tissues were cut, mounted onto glass slides, and coverslipped.

Estimation of the Spatial Resolving Power in A. albifrons Retina

The spatial resolving power was calculated based on the posterior nodal distance (PND) and the ganglion cell density according to Collin and Pettigrew [1989] to estimate the visual acuity of *A. albifrons*. Because the lens shape in *A. albifrons* was not spherical (see Results), it was not appropriate to apply the ratio of Matthiessen of 2.55, which has been commonly used to determine the PND in teleost fishes [Collin and Pettigrew, 1989]. Thus, for the calculation, we used average PND measured in the resin-embedded sections of 3 individuals whose total lengths (92.7, 97.5, and 106.4 mm) almost matched those of the individuals used for retinal ganglion cell topographical mapping (total lengths 93.3, 96.6, and 106.6 mm). The PND and ganglion cell density used to estimate the spatial resolving power were not corrected for shrinkage, because the fixation and dehydration processes required for tissue sectioning and the retinal flat mounting, which are the major causes of shrinkage, were almost identical.

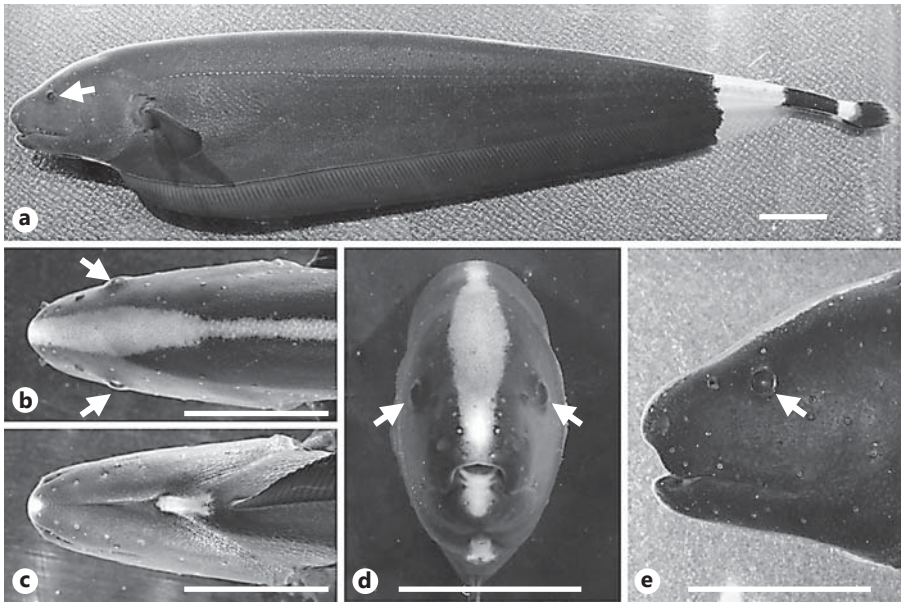

Fig. 1. External morphology of *A. albifrons*. **a** Photograph of the lateral view of the whole body. Photographs of the dorsal (**b**), ventral (**c**), frontal (**d**), and lateral (**e**) view of the head. The arrows indicate the position of the eyes. Scale bars = 10 mm.

Fig. 2. Anatomy of the eye in *A. albifrons*. **a** Photomicrograph of a horizontal section of the eye stained with toluidine blue and cut at the level of the optic nerve. EM = Extraocular muscle; NR = neural retina; ON = optic nerve; PD = pigmented dermal tissue. **b** Higher magnification of the retina showing the layered structures. BV = Blood vessel; GCL = ganglion cell layer; INL = inner nuclear layer; IPL = inner plexiform layer; NFL = nerve fiber layer; ONL = outer nuclear layer; OPL = outer plexiform layer; PE = pigment epithelium; PRL = photoreceptor layer. The arrow indicates a cluster of ganglion cells.

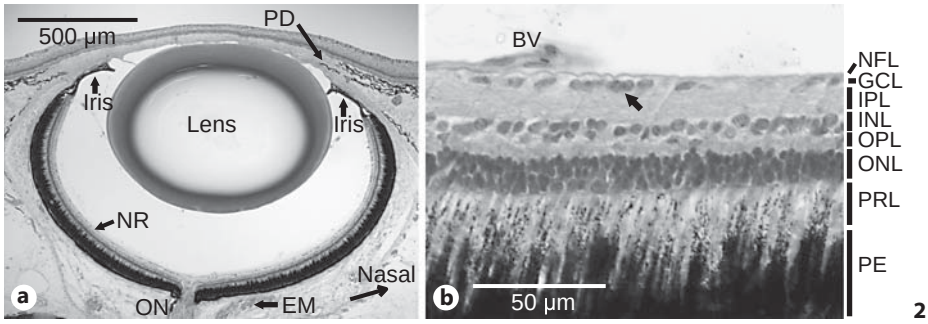

Results

Eye Morphology

Figures 1 and 2a show the external morphology of the head and a horizontal section of the *A. albifrons* eye crossing at the level of the exit of the optic nerve, respectively. Table 1 summarizes the numerical data of eye morphology in the individuals used for sectioning. The eye was almost embedded below the body surface (fig. 1, 2a), and the extraocular muscles were thin and not well developed (fig. 2a). No apparent foveal pit or depressed part of the retina was found. The lens was remarkably flattened and its width was approximately 22% greater than its thickness. It was apparent, together with the small amount of protrusion of the eye from the body surface, that the direction of incoming light was partially limited by the pigmented dermal tissues covering some peripheral parts of the pupil (fig. 1, 2a).

The layered structure of the *A. albifrons* retina displayed the general retinal features of vertebrates, while each layer was found to be poorly developed (fig. 2b). Ganglion cells did not form a continuous sheet of cell bodies, and the inner plexiform and optic nerve fiber layers were not clearly separated from each other in many parts of the retina (fig. 2b).

Retinal Ganglion Cell Distribution

The retinal flat-mount method developed in this study yielded sufficient quality to analyze the ganglion cell distribution over the retina. Table 2 lists various measures and calculation results obtained from flat-mounted retinae. The diameter of the eyeballs before dehydration was around 1.38 mm in the individuals used. The areas of the flat-mounted retinae were 3.45–3.91 mm^2, and the areal shrinkage of the tissue during the postfixation process was 3.12 ± 0.26% (mean ± SEM, n = 4).

Table 1. Summary of data on the body size, lens size, and PND of the 3 individuals of *A. albifrons* used for sectioning

	Total body length, mm	Lens width, mm	Lens thickness, mm	Lens flattening, %	PND, mm	
					nasal	temporal
Fish 1 (right eye)	92.7	0.95	0.70	26.3	0.69	0.71
Fish 2 (right eye)	97.5	0.90	0.71	21.1	0.68	0.60
Fish 3 (left eye)	106.4	1.04	0.81	22.1	0.75	0.72
Fish 3 (right eye)		1.00	0.82	17.9	0.74	0.69
Mean ± SEM	98.9±4.0	0.97±0.03	0.76±0.03	21.9±1.8	0.71±0.02	0.68±0.03

Measures, except for total body length, were obtained from resin-embedded preparations.

Table 2. Summary of the numerical data of the 3 individuals of *A. albifrons* used for retinal flat mounts and ganglion cell counting

	Total body length, mm	Eye diameter, mm	Retinal area, mm^2	Estimated total ganglion cells, n	Highest ganglion cell density, cells/mm^2		Estimated possible highest spatial resolving power, cycles/degree	
					nasal	temporal	nasal	temporal
Fish 1 (left eye)	93.3	1.34	3.45	7,851	3,900	3,600	0.57	0.54
Fish 2 (left eye)	96.6	1.39	3.52	5,866	3,300	2,600	0.53	0.46
Fish 3 (left eye)	106.6	1.41	3.91	9,081	4,400	4,100	0.57	0.59
Fish 3 (right eye)		NR	3.88	9,423	3,900	4,300	0.61	0.56
Mean±SEM	98.8±4.0	1.38±0.02	3.69±0.12	8,055±804	3,875±225	3,650±380	0.57±0.02	0.54±0.03

Measures of the eye diameter were obtained from fixed specimens before dehydration. Measures of the retinal area and the highest ganglion cell density were obtained from resin-embedded flat-mounted retinae. The total ganglion cell number was estimated from the areas of regions used for ganglion cell counting, the ganglion cell density in each region, and the retinal area. The estimated possible highest spatial resolving power was calculated from the highest ganglion cell density and the average posterior nodal distance in 3 individuals size-matched to individuals used for retinal flat mounts (see table 1). NR = Not recorded.

Figure 3 shows Nissl-stained ganglion cells in a flat-mounted retina. The cell bodies of the ganglion cells had irregular shapes and varied in size. Although it was not determined that all of the centrally projecting ganglion cells were located in the ganglion cell layer in *A. albifrons,* we presumed for later analyses that the major population of the retinal neurons projecting to the central nervous system consisted of neurons in the ganglion cell layer.

We also found that ganglion cells occasionally clustered (fig. 3) and that clusters were distributed over the whole retina. The clusters as well as ganglion cells independently distributed from the clusters were separated by wide gaps. This observation in flat-mounted retinae was consistent with that in sectioned preparations as shown in figure 2b. We found few putative displaced amacrine cells, which have small, circular, and densely stained profiles [Shand et al., 2000; Litherland et al., 2009; Muguru-

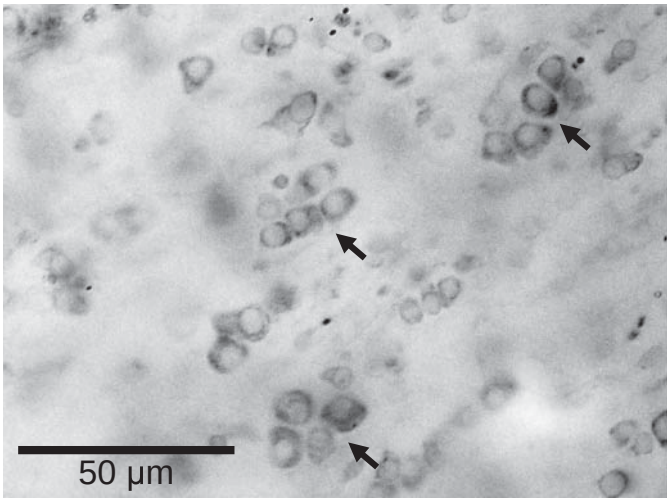

Fig. 3. Retinal ganglion cells in a flat-mounted retina. The arrows indicate clusters of ganglion cells.

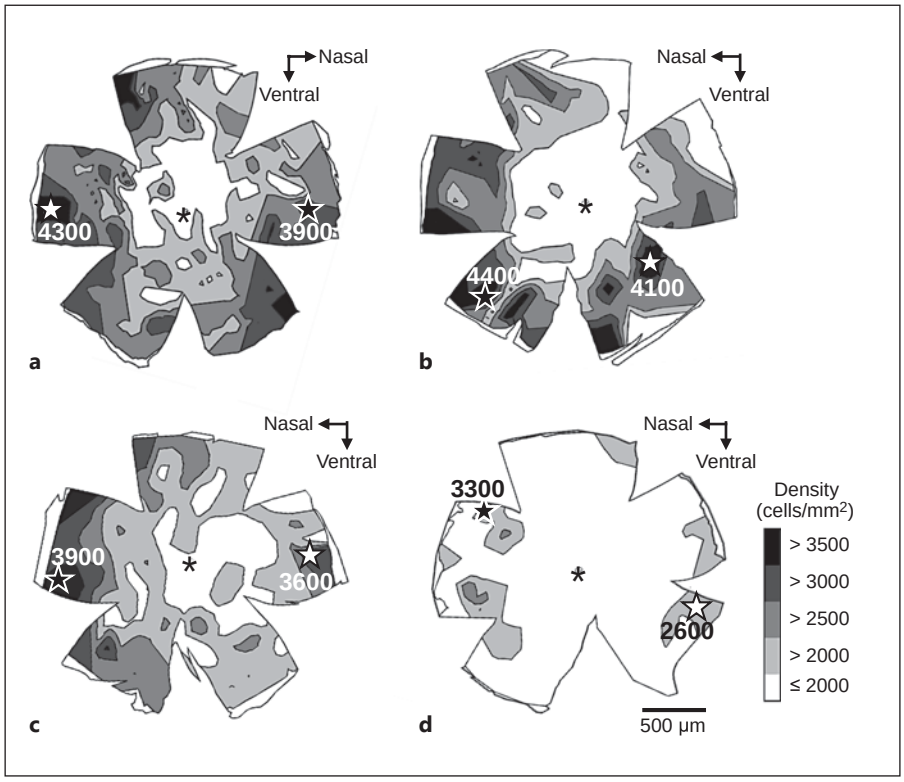

Fig. 4. Isodensity contour maps of retinal ganglion cells in 1 right (**a**) and 3 left (**b–d**) retinae from 3 individual *A. albifrons*. **a** and **b** were obtained from the same individual. Ganglion cells are distributed at high densities in the temporal and nasal areas of the retinae. Closed and open stars indicate the position of the highest ganglion cell density in the nasal and temporal portions of the retina, respectively. The number accompanying each star indicates the highest ganglion cell density. The asterisks indicate the position of the optic disks.

ma et al., 2013], in the ganglion cell layer in *A. albifrons*. Hence, we counted all Nissl-stained neural cells in the ganglion cell layer to investigate the ganglion cell distribution over the retina.

Figure 4 shows isodensity contour maps of the retinal ganglion cell distribution in *A. albifrons*. Ganglion cell densities were relatively high in the periphery and highest in the nasal and temporal regions. In 3 of the 4 retinae examined, ganglion cell densities were higher in the nasal region than in the temporal region, while the density was slightly higher in the temporal region in the remaining preparation (table 2). Topographic specialization was not so marked and showed a low specialization (approx. 3:1) with regard to cell gradients on the medionasal or mediotemporal axis. Furthermore, individual differences were high in terms of the peak and gradient of ganglion cell densities (fig. 4), although the regions of high ganglion cell densities were almost the same in the 4 retinae examined.

We estimated the highest possible spatial resolving power of the retina, assuming an image projected on the retina was in focus in the nasal and temporal regions where the ganglion cell density was the highest (fig. 4; table 2). The possible highest spatial resolving power was 0.57 ± 0.02 cycles/degree (mean ± SEM, n = 4) in the nasal peripheral region of the retina. In the temporal peripheral retina, where the ganglion cell density was also high (fig. 4; table 2), the estimated possible highest spatial resolving power was 0.54 ± 0.03 cycles/degree (mean ± SEM, n = 4).

Discussion

Modification of the Retinal Flat-Mount Method

In this study, we developed a modified retinal flat-mount method suitable for use with small eyes in juvenile fishes or less-developed eyes in some fish species. One of the characteristics of our method is postembedding removal of the pigment epithelium overlying the neural retina. In this way, we visualized the inner layers of the retina while avoiding fine surgical procedures or chemical bleaching, which are technically difficult to perform on very small and/or fragile specimens. In addition, since neural cells are stained before embedding, the progress of scraping of the outer layers can be checked under a light microscope during the procedure.

We successfully prepared retinal flat mounts of young *A. albifrons* with satisfactory qualities. It is relatively easy

to routinely make retinal flat-mount preparations of very small eyes (diameter <1 mm) and/or less developed eyes with thin retinae using our method. The shrinkage of the retinal tissue during the postfixation processes was comparable to that in the conventional retinal flat-mount method [Collin and Pettigrew, 1988; Mednick and Springer, 1988].

It has been shown for black bream *Acanthopagrus butcheri* and European hake *Merluccius merluccius* that the topographic arrangements of retinal ganglion cells vary as the fish grows and correlate with changes in their habitat and behavior [Shand et al., 1999, 2000; Bozzano and Catalán, 2002]. We believe that our method can extend the range of investigations of ontogenetic changes in retinal features to include earlier stages, as well as those in small or poorly developed eyes, and hence contribute to further understanding visual ecology in fish.

Visual Capability of A. albifrons

A prominent feature of the eye in *A. albifrons* is the flattening of the lens. Most teleost lenses are known to be nearly spherical [Sivak, 1990]. Thus, the unusually flattened lens in *A. albifrons* suggests that the eyes are underpowered [Munk, 1984], although focal properties cannot be determined based on lens shape alone [Sivak, 1990]. In addition, a case of well-developed acute vision in a teleost, the sandlance *Limnichthytes fasciatus,* which has flattened lenses, has also been reported as an exceptional case [Pettigrew and Collin, 1995]. In some sharks and stingrays, the width of the lens exceeds the thickness by more than 10% [Sivak, 1978]. Since the irises in some elasmobranch fishes are mobile and respond to changes in the level of illumination, elasmobranch flattened lenses might well have focal properties different from those of teleost spherical lenses [Sivak, 1990].

The extraocular muscles were found to be thin and the eyeball was almost embedded below the body surface, suggesting that the movement range of the eye is limited. These observations, together with the finding that pigmented dermal tissue partially covers the periphery of the pupil, suggest that the visible areas in this species are limited compared to other 'visual' fishes. Although the optic properties of the eye were not closely examined in this study, it is likely that this species has an inferior binocular visual capability. Nevertheless, we need to consider that this fish has elaborated a postural control ability. They can maintain posture with the lateral or ventral side up, and hence they can orient the visual axis towards various directions.

Although the layered structure of the retina in *A. albifrons* has the general retinal features found in other fishes [Powers and Easter, 1983; Wagner, 1990], each layer was found to be markedly poorly developed even compared to retinae in fishes such as the bottom-dwelling and nocturnal rufus snake eel *Ophichthus rufus* [Bozzano, 2003], the glass catfish *Kryptopterus bicirrhis* [Wagner, 1990], and the Japanese eel *Anguilla japonica* [Omura et al., 2003], in which the visual sense does not predominate over other modalities [Pankhurst and Lythgoe, 1983; Tomoda and Uematsu, 1996; Bozzano, 2003]. Additionally, we found no obvious specialized structures or arrangements in the photoreceptor layer adapted for dim light vision as seen in the African weakly electric fish *Gnathonemus petersii* [Landsberger et al., 2008].

Retinal ganglion cells in *A. albifrons* were sparsely distributed in the ganglion cell layer. It has been reported for the jawless fish (Agnatha) *Ichthyomyzon unicuspis* that 75% of retinal ganglion cells are located in the inner nuclear layer [Fritzsch and Collin, 1990]. Displacement of some ganglion cells to the inner nuclear layer has also been reported in the weakly electric fish *G. petersii* [Landsberger et al., 2008]. In this case, however, only some ganglion cell somata are displaced to the inner nuclear layer, and the vast majority of them are located in the ganglion cell layer [Landsberger et al., 2008]. Although it was not clear that all of the centrally projecting ganglion cells were located in the ganglion cell layer in *A. albifrons,* we presumed for further analysis that the major population of retinal neurons projecting to the central nervous system consist of neuronal cells in the ganglion cell layer.

The ganglion cells in *A. albifrons* showed occasional clustering and did not form a continuous sheet of cell bodies and the inner plexiform and optic nerve fiber layers were not clearly separated in many regions of the retina. Clustering of ganglion cells in relatively thin neural retinae has also been reported in some teleost fishes, including the glass catfish *K. bicirrhis* and the mooneye *Hiodon tergesius* [Wagner, 1990]. It is possible that the clustering has functional significance because it has been suggested that ganglion cells directly interact between themselves [Sakai et al., 1986].

The ganglion cell density was higher in the peripheral temporal and nasal regions of the retina. Given the location of specialization, visual acuity is relatively high in the frontal and temporocaudal directions, although the peak density gradient is as low as approximately 3:1 in terms of medionasal cell gradients.

The possible maximal spatial resolving power estimated based on the ganglion cell density and the PND actually measured in the sectioned eye was around 0.57 and 0.54 cycles/degree in the nasal and temporal retina, re-

spectively. This indicates that *A. albifrons* is one of the less-visual fishes. The estimated spatial resolving ability of the eye of *A. albifrons* appeared to be much lower than that of other fish species such as the rufus snake eel *O. rufus* [Bozzano, 2003] and the tripod fish *Bathypterois dubius* [Collin and Partridge, 1996], where the visual sense is not important compared to other senses. The estimated spatial resolving power in *O. rufus* has been reported to be 3.7–3.9 cycles/degree [Bozzano, 2003]. In *B. dubius,* although the spatial resolution was not calculated quantitatively, the peak ganglion cell density is over 7,000 cells/mm^2 in individuals in which retinae are larger than in the *A. albifrons* used in the present experiment, suggesting that the resolution is higher than in *A. albifrons* [Collin and Partridge, 1996]. However, as in humans, the minimum discriminability, or hyperacuity, can be higher than the minimum resolvable angle or ordinary acuity, which is primarily limited by the eye anatomy [Westheimer, 1981]. It has been reported in *A. albifrons* that some classes of tectal neurons respond well to moving-object stimuli close to the fish [Bastian, 1982]. Although blinded *A. albifrons* behave the same as sighted fish, vision has some role in locating objects in combination with other modalities of senses, especially electroreception [Bastian, 1982].

Strategies for prey capture in *A. albifrons* involve the utilization of multiple modalities of senses along the body to locate the prey and approach it using backward and forward movements [Nelson and Maciver, 1999]. It has also been demonstrated for the related species *A. leptorhynchus* that the best electric acuity for prey detection is situated in the middle of the body [Babineau et al., 2007]. Taken together, the most important region for prey detection is probably located along the side of the body. The nasal area centralis in the retina of *A. albifrons* could be used to locate prey close to the side of the body, and the fish then swims backwards to catch it. The maximal spatial resolving power of 0.57 cycles/degree in the nasal retina makes *A. albifrons* capable of visually detecting 1-mm prey, such as *Daphnia,* at about a 30-mm distance from the eye along the temporal, or caudal, visual axis. Using the hunting strategy mentioned above, it seems likely that the visual sense plays a role in the feeding behavior of this species in the wild.

It has been shown in 2 mormyrid species, i.e. *G. petersii* and *Brienomyrus niger,* that they are capable of an optomotor response [Teyssedre and Moller, 1982] and, at least in the former species, that vision can be a dominant sense in searching for prey when light is available [von der Emde and Bleckmann, 1998], although this African weakly electric fish possesses more-developed eyes [Landsberger et al., 2008] compared to *A. albifrons.* In addition, multiple sensory inputs including vision have been demonstrated to be integrated into spatial navigation in *G. petersii* [Rojas and Moller, 2002]. Furthermore, it has also been reported for *G. petersii* that there are individual differences in food-searching strategies and each individual favors a specific combination of sensory inputs [von der Emde and Bleckmann, 1998]. We found in *A. albifrons* that there were considerable individual differences in the peak density of ganglion cells but a shared pattern of topographic arrangement. This might reflect the individual preference of the strategy of foraging in *A. albifrons.*

In this study we revealed that *A. albifrons* possesses a very low visual capability compared to 'visual' fishes. However, we suggest that the eye in this species is not merely a luminance detector but is also functional for viewing the world with some acuity using specialized retinal areas.

Acknowledgement

We thank Drs. Naoyuki Yamamoto and Shiro Takei for their technical advice.

References

Albert JS (2003): Apteronotidae; in Reis RE, Kullander SO, Ferraris CJ Jr (eds): Checklist of the Freshwater Fishes of South and Central America. Porto Alegre, Edipucrs, pp 503–508.

Albert JS, Crampton WGR (2005). Diversity and phylogeny of neotropical electric fishes (Gymnotiformes); in Bullock TH, Hopkins CD, Popper AN, Fay RR (eds): Springer Handbook of Auditory Research. New York, Springer, pp 360–409.

Babineau D, Lewis JE, Longtin A (2007): Spatial acuity and prey detection in weakly electric fish. PLoS Comput Biol 3:e38.

Bastian J (1982): Vision and electroreception: integration of sensory information in the optic tectum of the weakly electric fish *Apteronotus albifrons.* J Comp Physiol A 147:287–297.

Bozzano A (2003): Vision in the rufus snake eel, *Ophichthus rufus:* adaptive mechanisms for a burrowing life-style. Mar Biol 143:167–174.

Bozzano A, Catalán IA (2002): Ontogenetic changes in the retinal topography of the European hake, *Merluccius merluccius:* implications for feeding and depth distribution. Mar Biol 141:549–559.

Browman HI, Gordon WC, Evans BI, O'Brien WJ (1990): Correlation between histologyical and behavioral measures of visual acuity in a zooplanktivorous fish, the white crappie *(Pomoxis annularis).* Brain Behav Evol 35:85–97.

Collin SP (2008): A web-based archive for topographic maps of retinal cell distribution in vertebrates. Clin Exp Optom 91:85–95.
Collin SP, Partridge JC (1996): Retinal specializations in the eyes of deep-sea teleosts. J Fish Biol 49:157–174.
Collin SP, Pettigrew JD (1988): Retinal ganglion cell topography in teleosts: a comparison between Nissl-stained material and retrograde labelling from the optic nerve. J Comp Neurol 276:412–422.
Collin SP, Pettigrew JD (1989): Quantitative comparison of the limits on visual spatial resolution set by the ganglion cell layer in twelve species of reef teleosts. Brain Behav Evol 34: 184–192.
Cox-Fernandes C (1998): Detrended correspondence canonical analysis (DCCA) of electric fishes assemblages in the Amazon; in Val AL, Almeida-Val VMF (eds): Biology of Tropical Fishes. Manaus, INPA, pp 21–39.
Fritzsch B, Collin SP (1990): Dendritic distribution of two populations of ganglion cells and the retinopetal fibers in the retina of the silver lamprey *(Ichthyomyzon unicuspis).* Vis Neurosci 4:533–545.
Giassi ACC, Maler L, Moreira JE, Hoffmann A (2011): Glomerular nucleus of the weakly electric fish, *Gymnotus* sp.: cytoarchitecture, histochemistry, and fiber connections – insights from neuroanatomy to evolution and behavior. J Comp Neurol 519:1658–1676.
Graydon ML, Giorgi PP (1984): Topography of the retinal ganglion cell layer of *Xenopus.* J Anat 139:145–157.
Hughes A (1971): Topographical relationships between the anatomy and physiology of the rabbit visual system. Doc Ophthalmol 30:33–159.
Hughes A (1977): The topography of vision in mammals of contrasting life style: comparative optics and retinal organization; in Crescitelli F (ed): Handbook of Sensory Physiology. Berlin, Springer, vol VII/5: The Visual System in Vertebrates, pp 613–756.
Landsberger M, von der Emde G, Haverkate D, Schuster S, Gentsch J, Ulbricht E, Reichenbach A, Makarov F, Wagner H-J (2008): Dim light vision – morphological and functional adaptations of the eye of the mormyrid fish, *Gnathonemus petersii.* J Physiol Paris 102: 291–303.
Lavoué S, Miya M, Arnegard ME, Sullivan JP, Hopkins CD, Nishida M (2012): Comparable ages for the independent origins of electrogenesis in African and South American weakly electric fishes. PLoS One 7:e36287.
Litherland L, Collin SP, Fritsches KA (2009): Eye growth in sharks: ecological implications for changes in retinal topography and visual resolution. Vis Neurosci 26:397–409.
Mangrum WI, Dowling JE, Cohen ED (2002): A morphological classification of ganglion cells in the zebrafish retina. Vis Neurosci 19:767–779.
Marrero C, Taphorn DC (1991): Notas sobre la historia natural y la distribución de los peces Gymnotiformes en la cuenca del Río Apure y otros ríos de la Orinoquia. Biollania 8:123–142.
Mednick AS, Springer AD (1988): Asymmetric distribution of retinal ganglion cells in goldfish. J Comp Neurol 268:49–59.
Moore BA, Kamilar JM, Collin SP, Bininda-Emonds ORF, Dominy NJ, Hall MI, Heesy CO, Johnsen S, Lisney TJ, Loew ER, Moritz G, Nava SS, Warrant E, Yopak KE, Fernández-Juricic E (2012): A novel method for comparative analysis of retinal specialization traits from topographic maps. J Vis 12:13.
Muguruma K, Takei S, Yamamoto N (2013): Retinal ganglion cell distribution and spatial resolving power in the Japanese catshark *Scyliorhinus torazame.* Zool Sci 30:42–52.
Munk O (1984): Non-spherical lenses in the eyes of some deep-sea teleosts. Arch Fisch Wiss 34: 145–153.
Nelson ME, Maciver MA (1999): Prey capture in the weakly electric fish *Apteronotus albifrons:* sensory acquisition strategies and electrosensory consequences. J Exp Biol 202:1195–1203.
Oliveira FG, Coimbra JP, Yamada ES, Montag LFDA, Nascimento FL, Oliveira VA, da Mota DL, Bittencourt AM, da Silva VL, da Costa BLDSA (2006): Topographic analysis of the ganglion cell layer in the retina of the four-eyed fish *Anableps anableps.* Vis Neurosci 23: 879–86.
Omura Y, Tstuzuki K, Sugiura M, Uematsu K, Tsukamoto K (2003): Rod cells proliferate in the eel retina throughout life. Fish Sci 69:924–928.
Pankhurst NW, Lythgoe JN (1983): Changes in vision and olfaction during sexual maturation in the European eel *Anguilla anguilla* (L.). J Fish Biol 23:229–240.
Pettigrew JD, Collin SP (1995): Terrestrial optics in an aquatic eye: the sandlance, *Limnichthytes fasciatus* (Creediidae, Teleostei). J Comp Physiol A 177:397–408.
Powers MK, Easter SS Jr (1983): Behavioral significance of retinal structure and function in fishes; in Northcut RG, Davis RE (eds): Fish Neurobiology. Ann Arbor, University of Michigan Press, vol 1: Brain Stem and Sense Organs, pp 377–404.
Rojas R, Moller P (2002): Multisensory contributions to the shelter-seeking behavior of a mormyrid fish, *Gnathonemus petersii* Günther (Mormyridae, Teleostei): the role of vision, and the passive and active electrosenses. Brain Behav Evol 59:211–221.
Rose GJ, Canfield JG (1993): Longitudinal tracking responses of the weakly electric fish, *Sternopygus*. J Comp Physiol A 171:791–798.
Sakai HM, Naka K-I, Dowling JE (1986): Ganglion cell dendrites are presynaptic in catfish retina. Nature 319:495–497.
Sas E, Maler L (1986): Retinofugal projections in a weakly electric gymnotid fish *(Apteronotus leptophynchus).* Neuroscience 18:247–259.
Shand J, Archer MA, Collin SP (1999): Ontogenetic changes in the retinal photoreceptor mosaic in a fish, the black bream, *Acanthopagrus butcheri.* J Comp Neurol 412:203–217.
Shand J, Chin SM, Harman AM, Moore S, Collin SP (2000): Variability in the location of the retinal ganglion cell area centralis is correlated with ontogenetic changes in feeding behavior in the black bream, *Acanthopagrus butcheri* (Sparidae, Teleostei). Brain Behav Evol 55:176–190.
Sivak JG (1978): Optical characteristics of the eye of the spiny dogfish *(Squalus acanthias).* Rev Can Biol 37:209–217.
Sivak JG (1990): Optical variability of the fish lens; in Douglas RH, Djamgoz MBA (eds): The Visual System of Fish. London, Chapman and Hall, pp 63–80.
Teyssedre C, Moller P (1982): The optomotor response in weak-electric mormyrid fish: can they see? Z Tierpsychol 60:306–312.
Tomoda H, Uematsu K (1996): Morphogenesis of the brain in larval and juvenile Japanese eels, *Anguilla japonica.* Brain Behav Evol 47:33–41.
Ullmann JFP, Moore BA, Temple SE, Fernández-Juricic E, Collin SP (2012): The retinal wholemount technique: a window to understanding the brain and behaviour. Brain Behav Evol 79: 26–44.
von der Emde G, Bleckmann H (1998): Finding food: senses involved in foraging for insect larvae in the electric fish *Gnathonemus petersii.* J Exp BIol 201:969–980.
Wagner H-J (1990): Retinal structure of fishes; in Douglas RH, Djamgoz MBA (eds): The Visual System of Fish. London, Chapman and Hall, pp 109–157.
Westheimer G (1981): Visual acuity; in Moses RA (ed): Adler's Physiology of the Eye: Clinical Application, ed 7. St. Louis, Mosby, pp 530–544.